The Journal of Immunology
RESEARCH ARTICLE | APRIL 01 2002

Segregation of Bad from Lipid Rafts Is Implicated in the Induction of Apoptosis[1] FREE

Verónica Ayllón; ... et. al

J Immunol (2002) 168 (7): 3387–3393.
https://doi.org/10.4049/jimmunol.168.7.3387

Segregation of Bad from Lipid Rafts Is Implicated in the Induction of Apoptosis[1]

Verónica Ayllón,* Aarne Fleischer,* Xavier Cayla,† Alphonse García,‡ and Angelita Rebollo[2]*

Many molecules relocate subcellularly in cells undergoing apoptosis. Using coimmunoprecipitation experiments we demonstrate that Bad is not associated to 14-3-3 protein, suggesting a new mechanism for the control of the proapoptotic role of Bad. Here we show, by confocal microscopy and cellular fractionation, that Bad is attached to lipid rafts in IL-4-stimulated cells and thymocytes while associated with mitochondria in IL-4-deprived cells. Disruption of lipid rafts by methyl-β-cyclodextrin treatment induces segregation of Bad from rafts, which correlates with apoptosis. Our results suggest that the interaction of Bad with rafts is a dynamic process regulated by IL-4 and involved in the control of apoptosis. ***The Journal of Immunology*****, 2002, 168: 3387–3393.**

Apoptosis is a highly conserved and essential feature of development and homeostasis in higher organisms. Progress has been made in identifying extracellular, intracellular, and cell surface molecules that regulate apoptosis. Interestingly, positive and negative regulators have been identified at each level.

The Bcl-2 family proteins act as a decision point in the apoptotic pathway. The family is divided into two functional groups: antiapoptotic members and proapoptotic members, including the BH3-only member Bad, which promote apoptosis (1). Bad shares identity only in the BH3 domain and forms heterodimers with Bcl-2 and Bcl-x. Upon stimulation of cells with IL-3 and NGF, Bad becomes serine phosphorylated, resulting in association with 14-3-3 protein (2, 3). It has been shown that the association of 14-3-3 protein with Bad is dependent on serine 155 phosphorylation of Bad. In agreement, IL-2-stimulation of a murine T cell line induces serine 112 and 136 phosphorylation of Bad without association with 14-3-3 protein (4).

Localization of proteins to distinct subcellular compartments, including membranes, is a critical event in multiple cellular pathways such as apoptosis. Plasma membranes of many cell types contain microdomains, commonly referred to as lipid rafts, that are biochemically distinct from bulk plasma membranes (5). These domains are enriched in sphingolipids and cholesterol, and they can be isolated by density gradient ultracentrifugation. In T cells, a number of proteins involved in signal transduction copurify with lipid rafts isolated on sucrose gradient (6, 7). Lipid rafts were visualized in intact cells by confocal microscopy using fluorescently labeled cholera toxin (CTx)[3] subunit B, which binds to the ganglioside GM1 (8). Disruption of raft integrity by a variety of methods inhibits early activation events, supporting a critical role for these domains in signaling.

Lipid rafts appear to play a central role in B cell activation. In mature B cells, signaling through the B cell Ag receptor is initiated from rafts and leads to activation. In immature B cells, B cell Ag receptor is excluded from rafts, and signaling leads to apoptosis (9–11). It has been shown that translocation and clustering of Fas into rafts triggers apoptosis in leukemic cells treated with the ether lipid ET-18-OCH(3) (12). In addition, Fas clustering in lipid rafts is a prerequisite for signaling and death (13, 14). CD24 induces apoptosis in human B cells via a raft-mediated signaling system (15). Finally, many receptors are inducibly localized in lipid rafts, which have been shown to function as platforms coordinating the induction of signaling pathways. The sequestration of IL-2R α-chain within lipid rafts restricts its intermolecular interactions and regulates IL-2R signaling through impeding its association with IL-2R β- and γ-chains (16). In this manuscript we identify for the first time the attachment sites in the plasma membrane for the apoptotic molecule Bad. We also show that interaction of Bad with rafts is an active process regulated by IL-4. We propose that segregation of Bad from rafts is involved in the induction of apoptosis.

Materials and Methods

Cells, lymphokines, and reagents

TS1αβ is a murine T cell line that can be propagated independently in IL-2, IL-4, or IL-9. Cells were cultured in RPMI 1640 as previously described (17). Murine rIL-4 or supernatant of a HeLa subline transfected with PKCRIL-4.neo was used as a source of murine IL-4. FITC-labeled CTx B subunit, CTx-biotin, and methyl-β-cyclodextrin (M-β-CD) were obtained from Sigma-Aldrich (St. Louis, MO). Cy3- and Cy2-conjugated secondary Abs were purchased from Molecular Probes (Eugene, OR). Anti-mitochondria serum (mito 2813, pyruvate dehydrogenase) was a gift from Dr. A. Serrano (Centro Nacional de Biotecnologia, Madrid, Spain).

Immunoprecipitation and Western blot

Cells (1×10^7) were IL-4-stimulated or -deprived and lysed for 20 min at 4°C in lysis buffer (50 mM Tris-HCl (pH 8), 1% Nonidet P-40, 137 mM NaCl, 1 mM $MgCl_2$, 1 mM $CaCl_2$, 10% glycerol, and protease inhibitor mixture). Lysates were immunoprecipitated with the corresponding Ab. Protein A-Sepharose was added for 1 h at 4°C, and after washing, immunoprecipitates were separated by SDS-PAGE. Alternatively, cells were lysed in Laemmli sample buffer, and protein extracts were separated by SDS-PAGE, transferred to nitrocellulose, blocked with 5% nonfat dry milk in TBS (20 mM Tris-HCl (pH 7.5) and 150 mM NaCl) and incubated with primary Ab in TBS/0.5% nonfat dry milk. Membranes were washed with 0.05% Tween 20 in TBS and incubated with peroxidase-conjugated secondary Ab. After washing, proteins were developed using the ECL system.

*Department of Immunology and Oncology, Centro Nacional de Biotecnología, Campus de Cantoblanco, Madrid, Spain; †Laboratoire de Physiologie de la Reproduction, Equipe Scientifique Associé Centre National de la Recherche Scientifique, Institut National de la Recherche Agronomique, and ‡Département d'Immunologie, Laboratoire de Signalisation Immunoparasitaire, Institut Pasteur, Paris, France

Received for publication November 28, 2001. Accepted for publication January 29, 2002.

The costs of publication of this article were defrayed in part by the payment of page charges. This article must therefore be hereby marked *advertisement* in accordance with 18 U.S.C. Section 1734 solely to indicate this fact.

[1] This work was supported in part by grants from the Association pour la Recherche sur le Cancer (ARC 4437) and Institut Pasteur (PTR-60). The Department of Immunology and Oncology was founded and is supported by the Spanish Research Council and Pharmacia Corp.

[2] Address correspondence and reprint requests to Dr. Angelita Rebollo, Department of Immunology and Oncology, Centro Nacional de Biotecnología, Campus de Cantoblanco, UAM 28049 Madrid, Spain. E-mail address: arebollo@cnb.uam.es

[3] Abbreviations used in this paper: CTx, cholera toxin; M-β-CD, methyl-β-cyclodextrin.

0022-1767/02/$02.00

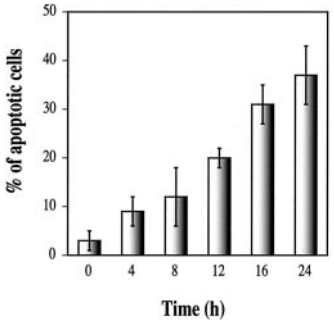

FIGURE 1. Effect of IL-4 deprivation on apoptosis. Cells were cultured in the presence of IL-4, deprived for the indicated times, and harvested. To analyze apoptosis, cells were diluted in ice-cold binding buffer, stained with annexin and propidium iodide, and analyzed by flow cytometry. The SD is shown where $n = 4$.

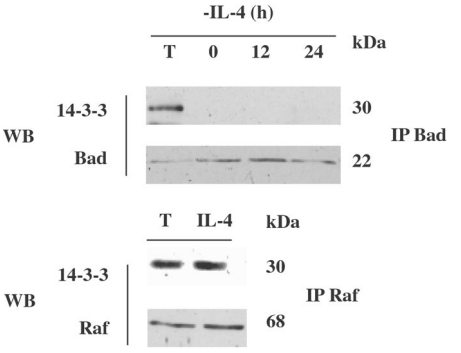

FIGURE 2. Effect of IL-4 on association of Bad with 14-3-3 protein. Cytoplasmic extracts from 10×10^6 IL-4-stimulated or -deprived cells were immunoprecipitated with anti-Bad or anti-Raf Abs and blotted with anti-14-3-3, anti-Raf, and anti-Bad. Total extracts (*lane T*) were used as a positive control of 14-3-3 and RAFT expression. Similar results were obtained in three independent experiments.

Cell cycle analysis

A total of 2×10^5 IL-4-stimulated cells treated with or without M-β-CD were washed, resuspended in PBS, permeabilized with 0.1% Nonidet P-40, and stained with 50 μg/ml propidium iodide. At different times, samples were analyzed using an EPICS XL flow cytometer (Coulter, Hialeah, FL). Apoptosis was measured as the percentage of cells in the sub-G_1 region of the fluorescence scale having a hypodiploid DNA content. Cell cycle was also analyzed by annexin staining. A total of 2×10^5 cells were washed with ice-cold PBS diluted in ice-cold binding buffer and stained with annexin and propidium iodide. Samples were maintained on ice for 10 min in the dark and then analyzed by flow cytometry.

Subcellular fractionation

Subcellular fractionation was performed as previously described (18, 19). Briefly, IL-4-stimulated or -deprived cells were washed in PBS and then resuspended for 2 min in extraction buffer STE (10 mM HEPES (pH 7.4), 1 mM EDTA, 0.25 mM sucrose, 2 μg/ml aprotinin, 10 μg/ml leupeptin, 1 mM PMSF, and 1 μg/ml pepstatin). The extract was inspected under the microscope, and >95% of the cells were lysed. The homogenates were applied to a linear gradient sucrose (0.73–1.9 M) and ultracentrifuged at $20{,}000 \times g$ overnight. The banded organelles were recovered by syringe, diluted with an equal volume of 10 mM HEPES buffer, and sedimented at the speed appropriated for the respective organelles. The purity of the organelles was determined by Western blot using Abs against specific markers: anti-cytochrome *c* for mitochondria, anti-Lck and CTx-biotin for rafts, anti-calnexin for endoplasmic reticulum, and anti-caspase 3 for cytosol. For preparation of cytosol, the homogenate was precentrifuged at $750 \times g$ for 10 min to remove nuclei and unbroken cells, followed by centrifugation at $100{,}000 \times g$ for 1 h to clear off the membranes.

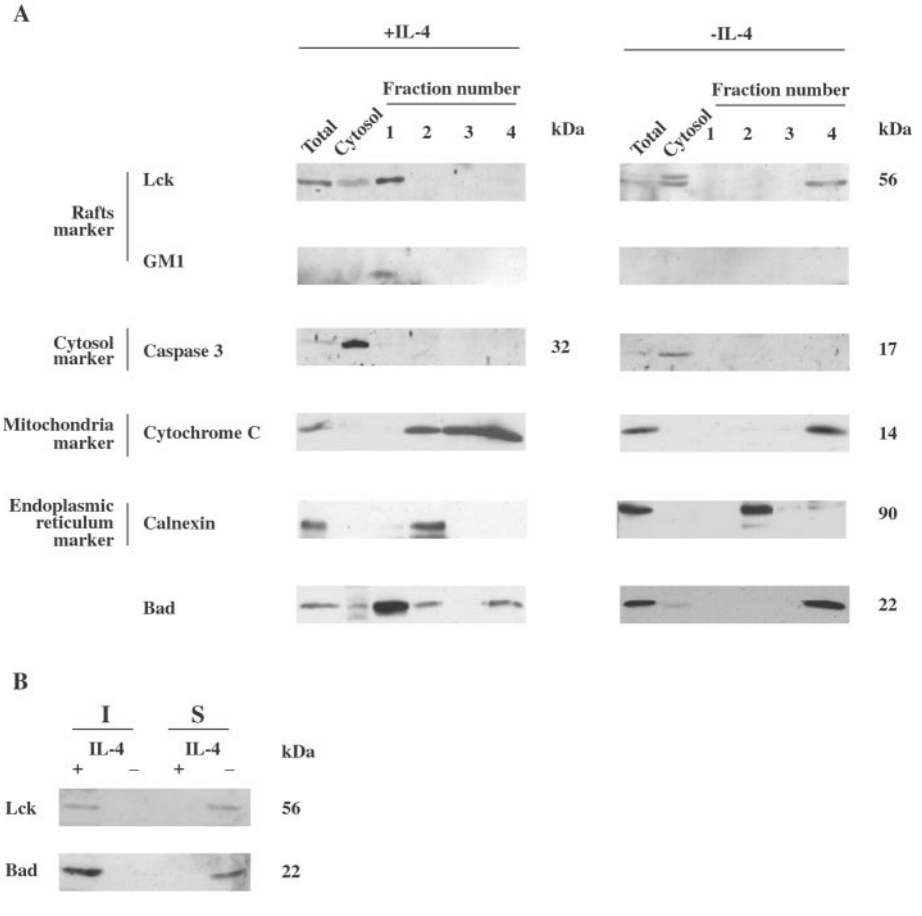

FIGURE 3. Subcellular localization of Bad in IL-4-stimulated or -deprived cells. *A*, Anti-Bad, anti-Lck (rafts), CTx-biotin (GM1 ganglioside, rafts), anti-caspase 3 (cytosol), anti-calnexin (endoplasmic reticulum), and anti-cytochrome *c* (mitochondria) immunoblot analysis of subcellular fractions from IL-4-stimulated or -deprived cells. The fractions (nos. 1–4) were prepared by sucrose gradient ultracentrifugation and tested for purity using Abs against mitochondria, rafts, endoplasmic reticulum, and cytosol. The nuclear fraction is not shown in the blot (fraction 5). The protein loaded per well in each gradient fraction corresponds to that of 5×10^6 cells. Total extracts contained 30 μg protein. Similar results were obtained in three independent experiments. *B*, IL-4-stimulated or -deprived cells were Triton X-100-extracted and fractionated in Optiprep flotation gradient. Fractions were collected from the top to the bottom of the gradient and were analyzed by Western blot. Only the first, insoluble proteins (I) and the last fraction, soluble proteins (S) are shown. Similar results were obtained in two independent experiments.

CTx-FITC labeling

IL-4-stimulated or -deprived cells were fixed with 1% paraformaldehyde for 5 min on ice, permeabilized, and then incubated with CTx-FITC (20 min, 6 μg/ml) and anti-Bad Ab for 1 h in PBS-BSA. Cy3-labeled secondary Ab was added and incubated for 1 h. Finally, and after several washing steps, cells were incubated with methanol at −20°C for 10 min, mounted with Vectashield medium, and analyzed by confocal microscopy. The program used for quantification of samples was Leica TSC NT version 1.5.451 (Leica, Lasertechnik, Heidelberg, Germany).

Cholesterol depletion

IL-4-stimulated serum-deprived cells were treated for 30 min at 37°C with 10 mM M-β-CD, washed, and then incubated with CTx-FITC and anti-Bad or anti-Lck Abs as described above. Secondary Ab was added and incubated for 1 h. Finally, cells were incubated with methanol at −20°C for 10 min and mounted as described above.

Triton X-100 flotation

IL-4-stimulated or -deprived cells were lysed in TXNE buffer (50 mM Tris-HCl (pH 7.4), 150 mM NaCl, 5 mM EDTA, and 0.2% Triton X-100) containing protease inhibitor mixture. Detergent-insoluble membranes were isolated by ultracentrifugation (17,000 × *g*, 4 h, 4°C) in a 30–35% gradient of Optiprep as previously described (Sigma-Aldrich, St. Louis, MO) (20).

Isolation of mitochondria and S-100 fraction

Mitochondria were isolated using a modification of the method described by Yang et al. (21). Briefly, 20×10^6 cells were IL-4-stimulated or -deprived, harvested, and washed with ice-cold PBS. Cell pellet was suspended in 5 vol ice-cold buffer A (20 mM HEPES-KOH (pH 7.5), 10 mM KCl, 1.5 mM $MgCl_2$, 1 mM EDTA, 1 mM EGTA, 1 mM DTT, 0.1 mM PMSF, and 250 mM sucrose) supplemented with protease inhibitors. Cells were disrupted in a Dounce homogenizer (Kontes, Vineland, NJ), the nuclei were centrifuged (1,000 × *g*, 10 min, 4°C), and the supernatant was further centrifuged (10,000 × *g*, 15 min, 4°C). The resulting mitochondrial pellet was resuspended in buffer A and stored at −80°C. The supernatant was centrifuged (100,000 × *g*, 1 h, 4°C), and the resulting S-100 fraction was stored at −80°C.

Results

Bad associates with lipid rafts in IL-4-stimulated cells

We have previously reported that Bcl-2 is expressed in IL-2-stimulated cells and Bcl-x in IL-4-cultured cells (22). When IL-4-maintained cells are deprived of lymphokine, they undergo apoptosis (Fig. 1). As early as 4 h after IL-4 deprivation, ~9% of the cells were apoptotic, reaching 40% at 24 h, whereas control IL-4-stimulated cells showed no significant level of apoptosis.

It has been shown that after IL-3-stimulation, Bad becomes phosphorylated, resulting in association with 14-3-3 protein. We have recently shown that IL-2 induces Bad phosphorylation, but not association with 14-3-3 protein (4). Fig. 2 shows that neither IL-4-stimulation nor IL-4-deprivation results in association of Bad to 14-3-3 protein. As an internal control, the interaction of Raf and the 14-3-3 protein is shown (Fig. 2).

Given that localization of proteins to distinct subcellular compartments is a critical event in multiple cellular pathways, comprising apoptosis, we analyzed the subcellular distribution of Bad in IL-4-stimulated or -deprived cells. IL-4-stimulated or -deprived cells were lysed and fractionated over sucrose gradient. To validate our gradient protocol, fractions (nos. 1–4) were immunoblotted with markers for rafts (Lck and GM1 ganglioside), mitochondria (cytochrome *c*), endoplasmic reticulum (calnexin), and cytosol (caspase 3). Nuclear fraction (5) is not shown in the blot, because there is no Bad localization in the nucleus. Rafts were detected by Western blot in fraction 1 using anti-Lck Ab and CTx-biotin, which recognizes GM1 ganglioside (Fig. 3*A*). Most Bad was found in rafts (fraction 1), although a very small fraction was also present in mitochondria (fraction 4), and cytosol and endoplasmic reticulum (fraction 2). As an internal control, Bad was observed in total extracts of IL-4-stimulated cells. Finally, we have observed that the fraction of Bad that is sequestered in lipid rafts is dephosphorylated (data not shown).

IL-4-deprivation induces disorganization of rafts (fraction 1), which are not detected using either anti-Lck Ab or CTx-biotin. The mitochondria marker, which also contains other cellular structures with similar density, is observed in fraction 4, and most caspase 3 is cleaved, given a new protein of lower m.w. More interesting, Bad is almost undetectable in cytosol and rafts and is only observed in fraction 4, which corresponds to mitochondria and cellular structures with similar densities (Fig. 3*A*). This result strongly suggests an IL-4-dependent association of Bad with rafts and translocation to mitochondria upon IL-4 deprivation. We also isolated rafts by Triton X-100 flotation gradient. As shown in Fig. 3*B*, Bad and Lck are detected in the detergent-insoluble fraction (I) of IL-4-stimulated cells, which corresponds to lipid rafts. In IL-4-deprived cells, Bad and Lck are detected in the fraction corresponding to soluble proteins (S). We have observed that post-translational myristoylation targets Bad to rafts (data not shown).

The subcellular localization of Bad was also analyzed in mitochondrial and cytosolic fractions of IL-4-stimulated or -deprived cells. Bad was detected in the mitochondrial fraction of IL-4-stimulated cells (Fig. 4*A*). The amount of Bad associated with mitochondria increased upon IL-4 deprivation. Traces of Bad were detected in the cytosolic fraction of IL-4-stimulated or -deprived cells. The antiapoptotic molecule Bcl-x_L was weakly detected in the mitochondrial fraction of IL-4-stimulated cells, increasing after

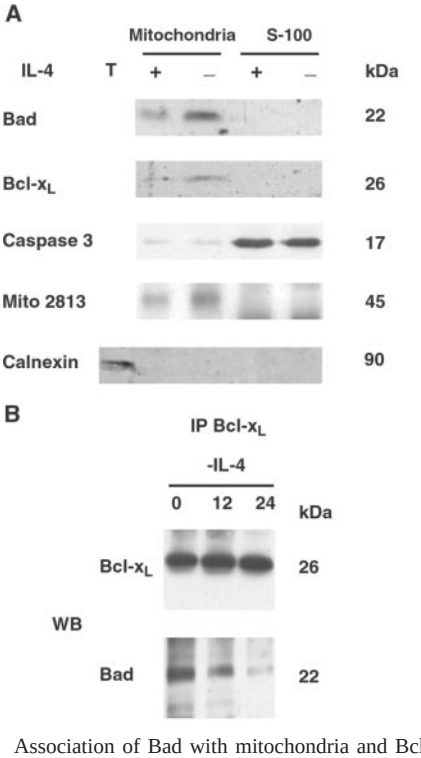

FIGURE 4. Association of Bad with mitochondria and Bcl-x_L. *A*, Mitochondrial and cytosolic proteins were isolated from IL-4-stimulated or -deprived cells, separated by SDS-PAGE, transferred to nitrocellulose, and immunoblotted with anti-Bad, anti-Bcl-x_L, anti-caspase 3 (cytosolic marker), anti-mitochondria Mito 2813 (pyruvate dehydrogenase, mitochondria marker), and anti-calnexin (endoplasmic reticulum marker). Protein bands were detected using the ECL system. Similar results were obtained in three independent experiments. *B*, Cytoplasmic lysates from IL-4-stimulated or -deprived cells were immunoprecipitated with anti-Bcl-x_L, transferred to nitrocellulose, and blotted with anti-Bad and anti-Bcl-x_L Abs. Protein bands were detected as described in *A*. Similar results were obtained in three independent experiments.

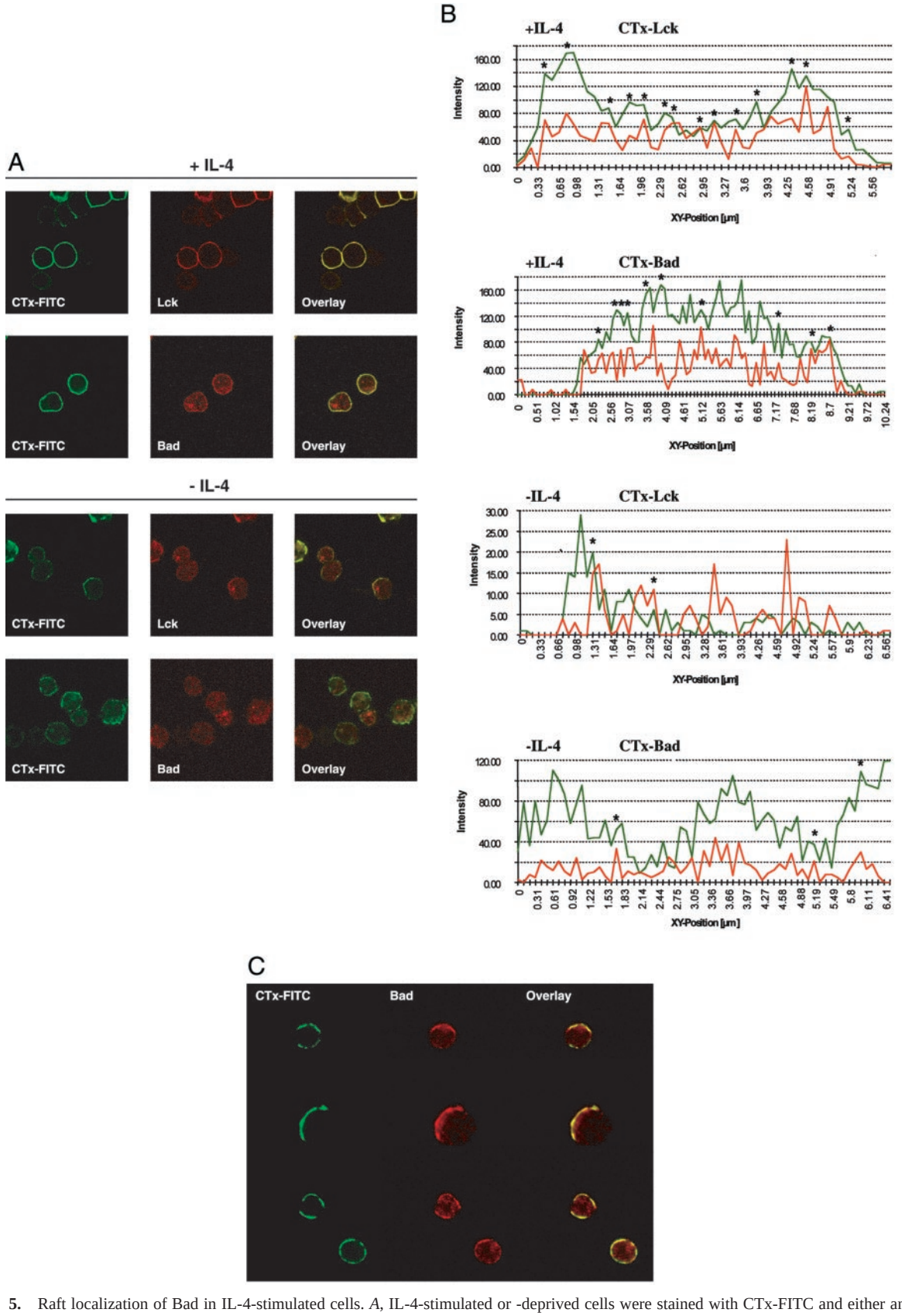

FIGURE 5. Raft localization of Bad in IL-4-stimulated cells. *A*, IL-4-stimulated or -deprived cells were stained with CTx-FITC and either anti-Lck or anti-Bad Abs as indicated, followed by Cy3-labeled secondary Ab, and were analyzed by confocal microscopy. Similar results were obtained in three independent experiments. Single confocal sections show fluorescence in green (FITC) and red (Cy3). *B*, The profile of green and red fluorescence colocalization in a surface of the cell membrane was analyzed using quantification software (Leica). The peaks of fluorescence colocalization are labeled with stars. *C*, Freshly isolated thymocytes from mice were stained as described in *A*, followed by Cy3-labeled secondary Ab, and analyzed by confocal microscopy. Similar results were obtained in two independent experiments.

IL-4 deprivation. As an internal control of protein fractionation, the blot was probed with anti-caspase 3 (cytosolic marker), anti-mitochondria Mito 2813 (pyruvate dehydrogenase, mitochondrial marker), and anti-calnexin to show the lack of endoplasmic reticulum contamination in mitochondrial preparation. Total extracts (*lane T*) were used as a positive control of calnexin expression. Finally, we explored the association of Bad with some Bcl-2 family members. We performed coimmunoprecipitation experiments of cytoplasmic proteins under IL-4 stimulation or deprivation conditions using specific Abs. Bad was detected by Western blot in anti-Bcl-x_L immunoprecipitates of IL-4-stimulated cells, decreasing throughout the starvation period analyzed (Fig. 4*B*). Probing the membrane with anti-Bcl-x_L Ab showed similar levels in all analyzed conditions.

Bad association with rafts in IL-4-stimulated cells was also analyzed in intact cells by confocal microscopy (Fig. 5*A*). IL-4-stimulated or -deprived cells were incubated with the raft marker CTx B subunit (CTx-FITC) before secondary labeling with anti-Bad or anti-Lck Ab. Double-immunofluorescence analysis with anti-Bad and CTx-FITC showed raft localization of Bad in the surface of IL-4-stimulated cells. In marked contrast, we observed a disorganization of rafts in IL-4-deprived cells and consequently no raft localization of Bad in IL-4-deprived cells (Fig. 5*A*). Double-immunofluorescence analysis with anti-Lck and CTx-FITC was used as a positive control of localization of Lck in membrane rafts of IL-4-stimulated cells. We did not detect Lck associated with rafts in IL-4-deprived cells (Fig. 5*A*). The profile of green and red fluorescence colocalization was analyzed using the quantification software of Leica (TCS NT; Leica, Rockleigh, NJ). As shown in Fig. 5*B*, a high number of green and red colocalization peaks was observed in the membrane of IL-4-stimulated cells stained with CTx-Lck or CTx-Bad. On the contrary, the level of colocalization of green and red fluorescence was strongly reduced in IL-4-deprived cells (Fig. 5*B*). This result suggests that Bad is preferentially localized in lipid rafts in IL-4-stimulated cells and segregates from plasma membrane in IL-4-deprived cells. Similar results of colocalization of Bad with lipid rafts were observed using freshly isolated thymocytes from mice (Fig. 5*C*).

Bad association with mitochondria in IL-4-deprived cells was also analyzed in intact cells by confocal microscopy (Fig. 6*A*). Double-immunofluorescence analysis with anti-Bad and anti-mitochondria Abs shows weak association of Bad to mitochondria in IL-4-stimulated cells, while there is a high fraction of Bad associated with mitochondria in IL-4-deprived cells (Fig. 6*A*). This separation of Bad from rafts correlates with its translocation to mitochondria in IL-4-deprived cells, as shown by cellular fractionation and confocal microscopy (Fig. 3*A*). The profile of green and red fluorescence colocalization was also analyzed using quantification software (Leica). Fig. 6*B* shows moderate green and red colocalization peaks in IL-4-stimulated cells stained with anti-Bad and anti-mitochondria Abs. The level of colocalization of both fluorescences strongly increases in IL-4-deprived cells (Fig. 6*B*).

Association of Bad with lipid rafts is required for prevention of apoptosis

Depletion of cellular cholesterol impairs the ability of glycosyl phosphatidylinositol-anchored proteins to associate with lipid rafts. To examine whether there is a similar requirement of cholesterol for the association of Bad with rafts, IL-4-stimulated cells were treated for 30 min with or without 10 mM M-β-CD in serum-free medium to deplete cellular cholesterol. Cells were then incubated with CTx-FITC and labeled with anti-Bad or anti-Lck Abs. Serum depletion alone weakly disrupted the association of Lck or Bad with lipid rafts (Fig. 7*A*). However, M-β-CD treatment caused a severe disruption of raft formation and association of Lck and Bad with rafts in IL-4-stimulated cells (Fig. 7*A*). This result indicates that disruption of raft formation by cholesterol depletion induces segregation of Bad and Lck from rafts in IL-4-stimulated cells. The profile of green and red fluorescence colocalization in control or M-β-CD-treated cells is shown in Fig. 7*B*. Background staining with secondary Abs, anti-rabbit Cy3, or anti-mouse Cy3 is shown in Fig. 7*C*.

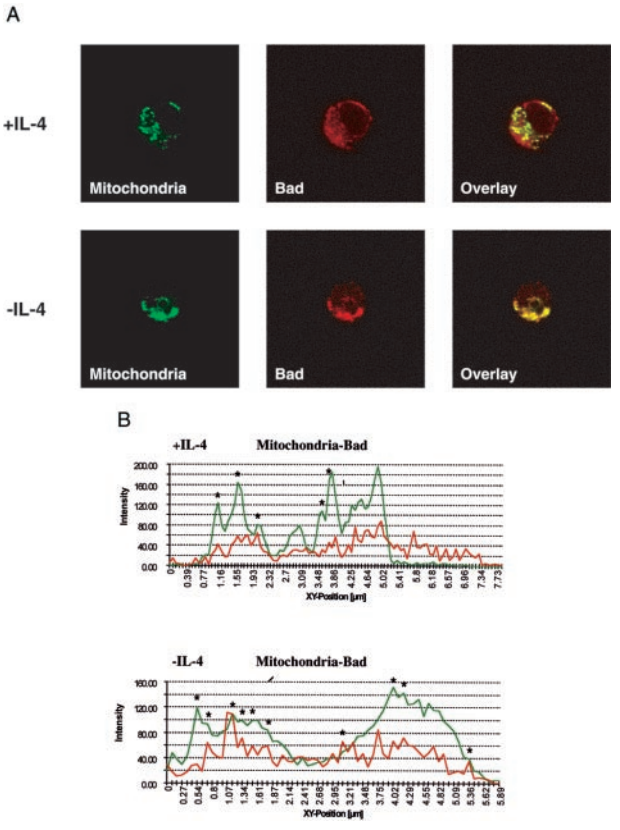

FIGURE 6. Mitochondrial localization of Bad. IL-4-stimulated or -deprived cells were stained with anti-Bad and anti-mitochondria Abs, followed by FITC- and Cy3-labeled secondary Abs, and analyzed as described above. Similar results were obtained in three independent experiments. *B*, The profile of green and red fluorescence colocalization in a surface of the cell membrane was analyzed using quantification software (Leica). The peaks of fluorescence colocalization are labeled with stars.

Given that exclusion of Bad from rafts was also observed in apoptotic IL-4-deprived cells (Fig. 5*A*), we analyzed whether Bad association with rafts and its integrity were necessary for prevention of apoptosis. For this purpose, IL-4-stimulated cells were treated for 30 min with or without M-β-CD in serum-free medium, then washed, resuspended in IL-4-supplemented complete medium, and analyzed for induction of apoptosis at different times (Fig. 8). M-β-CD-treated cells showed a stronger level of apoptosis compared with control nontreated cells, reaching the highest level 5 h after M-β-CD treatment. Eight hours after treatment the amounts of apoptotic cells detected in treated and nontreated cells were similar, because addition of serum restores the lipid composition of the membrane (data not shown). This result suggests that segregation of Bad from rafts is involved in the induction of apoptosis.

Discussion

Subcellular localization of Bad let us analyze how Bad function may be regulated by dynamic interaction with lipid rafts or mitochondria. The distinct Bad distribution and function are directly related to IL-4 stimulation or deprivation of the cells.

Our data show that 14-3-3 protein does not control the proapoptotic role of Bad. On the basis of this result, we analyzed the

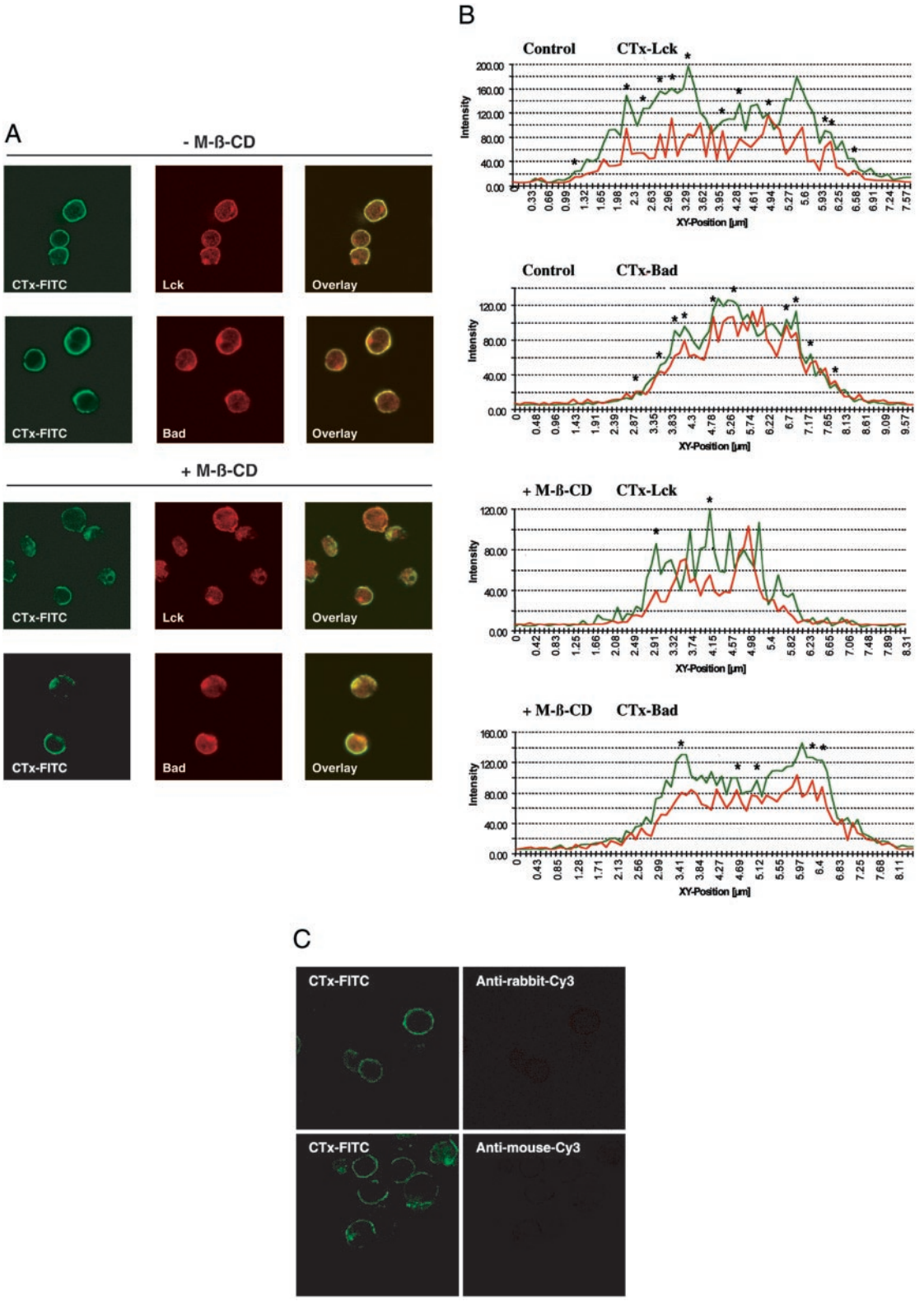

FIGURE 7. M-β-CD treatment abolishes association of Bad with rafts. *A*, IL-4-stimulated cells were serum-starved for 30 min and then treated with or without 10 mM M-β-CD for 30 min at 37°C before incubation with CTx-FITC and anti-Bad or anti-Lck Abs, followed by Cy3-labeled secondary Ab. Then cells were analyzed by confocal microscopy. Similar results were obtained in two independent experiments. Single confocal sections show green (FITC) and red (Cy3) fluorescence. *B*, The profile of green and red fluorescence colocalization in a surface of the cell membrane was analyzed using quantification software (Leica). The peaks of fluorescence colocalization are labeled with stars. *C*, Background staining with anti-rabbit Cy3 or anti-mouse Cy3.

subcellular distribution of Bad in IL-4-stimulated or -deprived cells, because localization of proteins is an important event in apoptosis. Our results show that different plasma membrane fractions can be separated using a subcellular fractionation sucrose ultracentrifugation gradient, because raft markers were successfully resolved from non-raft markers. We also isolated

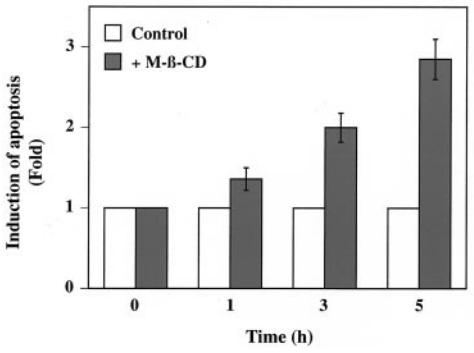

Time	Apoptotic cells (%) Control	+ M-ß-CD	Induction of apoptosis (Fold)
0 h	27,5 ± 2,5	28,5 ± 1,5	1 ± 0,0
1 h	17 ± 2	24,5 ± 1,5	1,4 ± 0,1
3 h	12 ± 4	24 ± 4	2 ± 0,2
5 h	5,5 ± 0,5	15,5 ± 0,5	2,9 ± 0,2

FIGURE 8. M-β-CD treatment induces apoptosis. IL-4-stimulated cells were serum-starved for 30 min, then treated with or without 10 mM M-β-CD for 30 min at 37°C, washed, and transferred to complete medium supplemented with IL-4. At different times, apoptosis was measured. The sub-G_1 region of the fluorescence scale was used to determine the percentage of cells present in the initial step of apoptosis. Similar results were obtained in two independent experiments. □, control cells; ■, M-β-CD-treated cells.

rafts and mitochondria by Triton X-100 flotation gradient and differential centrifugation, respectively. There are precedents for reversible raft association, as has been shown following the movement of single-fluorescence lipid molecules (23). In addition, after activation by ligand binding the epidermal growth factor migrates out of rafts into bulk plasma membrane (24). The association of proteins with lipid rafts can be modulated, because some proteins may be excluded from rafts by association with other proteins (25). Association of Bad with rafts may be involved in steps leading to Bad inactivation, because rafts do not constitute the final site of activation. IL-4 deprivation induces the segregation of Bad from rafts. This result suggests a two-step apoptotic process: segregation of Bad from rafts, which triggers apoptosis, and disorganization of lipid rafts during the apoptotic process. This is strongly suggested by results showing that disruption of cholesterol-rich rafts prevents Bad association and induces apoptosis in IL-4-stimulated M-β-CD-treated cells. Addition of FCS to IL-4-supplemented medium restores the lipid components of the plasma membrane, preventing the progression of apoptosis.

Localization of proteins to distinct subcellular fractions is an essential step in multiple signaling pathways, including apoptosis. According to this, it has been shown that some signaling molecules are sequestered in rafts. Cholesterol depletion disrupts lipid rafts and modulates the activity of multiple signaling pathways in T lymphocytes (26). Our results strongly suggest that in the absence of association of Bad to 14-3-3 protein, Bad is sequestered in rafts, avoiding a proapoptotic role and association with partners. IL-4 deprivation-induced segregation of Bad from rafts correlates with translocation to mitochondria and induction of apoptosis. Restriction of intermolecular interactions by sequestration in lipid rafts has been also described for the α-chain of the IL-2R, avoiding its association with the β- and γ-chains of the IL-2R (16). We show for the first time the sequestration of Bad into lipid rafts as an IL-4-dependent mechanism that controls the availability of proapoptotic Bad.

References

1. Downward, J. 1999. How BAD phosphorylation is good for survival. *Nat. Cell. Biol. 1:33.*
2. Hsu, H. Y., L. Kaipai, L. Zhu, and A. J. Hsueh. 1997. Interference of Bad-induced apoptosis in mammalian cells by 14-3-3 isoforms and P11. *Mol. Endocrinol. 11:1858.*
3. Yang, E., J. Zha, E. J. Jockel, L. H. Boise, C. B. Thompson, and S. J. Korsmeyer. 1995. Bad, a heterodimeric partner for Bcl-x_L and Bcl-2, displaces Bax and promotes cell death. *Cell 80:285.*
4. Ayllón, V., X. Cayla, A. Garcia, F. Roncal, R. Fernandez, J. P. Albar, C. Martinez, and A. Rebollo. 2001. Bcl-2 targets protein phosphatase 1α to Bad. *J. Immunol. 166:7345.*
5. Brown, D. A., and E. London. 1998. Functions of lipid rafts in biological membranes. *Annu. Rev. Cell. Dev. Biol. 14:111.*
6. Langlet, C., A. M. Bernard, P. Drevot, and H. Y. He. 2000. Membrane rafts and signaling by the multichain immune recognition receptors. *Curr. Opin. Immunol. 12:250.*
7. Anderson, H. A., E. M. Hiltbold, and P. A. Roche. 2000. Concentration of MHC class II molecules in lipid rafts facilitates antigen presentation. *Nat. Immunol. 2:156.*
8. Harder, T., P. Scheiffele, P. Verkade, and K. Simons. 1998. Lipid domain structure of the plasma membrane revealed by patching of membrane components. *J. Cell Biol. 141:929.*
9. Cheng, P. C., M. L. Dykstra, R. N. Mitchel, and S. K. Pierce. 1999. A role for lipid rafts in BCR signaling and antigen targeting. *J. Exp. Med. 190:1549.*
10. Aman, M. J., and K. S. Ravichandran. 2000. A requirement for lipid rafts in B cell receptor induced Ca^{++} flux. *Curr. Biol. 10:393.*
11. Petrie, R. J., P. P. Schnetkamp, K. D. Patel, M. Awasthi-Kalia, and J. P. Deans. 2000. Transient translocation of the B cell receptor and Src homology 2 domain-containing inositol phosphatase to lipid rafts: evidence toward a role in calcium regulation. *J. Immunol. 165:1220.*
12. Gajate, C., and F. Mollinedo. 2001. The antitumor ether lipid ET-18-OCH(3) induces apoptosis through translocation and capping of Fas/CD95 into membrane rafts in human leukemic cells. *Blood 98:3860.*
13. Grassme, H., A. Jekle, A. Richle, H. Schwarz, J. Berger, K. Sandhoff, R. Kolesnick, and E. Gulbins. 2001. CD95 signaling via ceramide rich membrane rafts. *J. Biol. Chem. 276:20589.*
14. Grassme, H., V. Jendrossek, J. Block, A. Reihle, and E. Gulbins. 2002. Ceramide-rich membrane rafts mediate CD40 clustering. *J. Immunol. 168:298.*
15. Suzuki, T., N. Kiyokawa, T. Taguchi, T. Sekino, Y. Katagiri, and J. Fujimoto. 2001. CD24 induces apoptosis in human B cells via the glycolipid-enriched membrane domains/rafts-mediated signaling system. *J. Immunol. 166:5567.*
16. Marmor, M., and M. Julius. 2001. Role of lipid rafts in regulating IL-2 receptor signaling. *Blood 98:1489.*
17. Pitton, C., A. Rebollo, J. Van Snick, J. Theze, and A. Garcia. 1993. High affinity and intermediate affinity forms of the IL-2R expressed in an IL-9-dependent murine T cell line deliver proliferative signals via differences in their transduction pathways. *Cytokine 5:362.*
18. Hacki, J., L. Egger, L. Monney, S. Coms, T. Rosse, I. Fellay, and C. Borner. 2000. Apoptotic crosstalk between the endoplasmic reticulum and mitochondria. *Oncogene 19:2286.*
19. Millan, J., and M. A. Alonso. 1998. MAL, a novel integral membrane protein of human T lymphocytes, associates with glycosylphosphatidylinositol-anchored proteins and Src-like tyrosine kinases. *Eur. J. Immunol. 28:3675.*
20. Mañes, S., E. Mira, C. Gomez, R. Lacalle, P. Keller, P. Labrador, and C. Martinez-A. 1999. Membrane rafts mediate front-rear polarity migrating cells. *EMBO J. 18:6211.*
21. Yang, J., X. Liu, K. Bhalla, C. N. Kim, A. M. Ibarro, J. Cai, T. Peng, D. P. Jones, and X. Wang. 1997. Prevention of apoptosis by Bcl-2: release of cytochrome *c* from mitochondria. *Science 275:1129.*
22. Gomez, J., C. Martinez-A, A. Gonzalez, and A. Rebollo. 1998. Bcl-2 is differentially regulated by IL-2 and IL-4: role of the transcription factor NFAT. *Oncogene 17:1235.*
23. Schutz, G. J., G. Kada, V. P. Pastushenko, and H. Schindler. 2000. Properties of lipid microdomains visualized by single molecule microscopy. *EMBO J. 19:892.*
24. Mineo, C., G. N. Gill, and R. W. Anderson. 1999. Regulated migration of epidermal growth factor receptor from caveolae. *J. Biol. Chem. 274:30636.*
25. Field, K. A., D. Holowka, and B. Baird. 1995. FcRI-mediated recruitment of p53/p56^{lyn} to detergent resistant membrane domains accompanies cellular signaling. *Proc. Natl. Acad. Sci. USA 92:9201.*
26. Kabouridis, P. S., J. Janzen, A. L. Magee, and S. C. Ley. 2000. Cholesterol depletion disrupts lipid rafts and modulates the activity of multiple signaling pathways in T cells. *Eur. J. Immunol. 30:954.*